SCIENTIFIC REPORTS

OPEN

TiO_2 nanoparticles induce omphalocele in chicken embryo by disrupting Wnt signaling pathway

Received: 8 December 2017
Accepted: 5 March 2018
Published online: 19 March 2018

Shweta Patel[1], Sarmita Jana[1], Rajlakshmi Chetty[3], Sonal Thakore[2], Man Singh[3] & Ranjitsinh Devkar[1]

Titanium dioxide nanoparticles (TiO_2 NPs) are among abundantly used metal oxide NPs but their interactions with biomolecules and subsequent embryonic toxicity in higher vertebrates is not extensively reported. Physicochemical interactions of TiO_2 NPs with egg albumen reveals that lower doses of TiO_2 NPs (10 and 25 µg/ml) accounted for higher friccohesity and activation energy but an increment in molecular radii was recorded at higher doses (50 and 100 µg/ml). FTIR analysis revealed conformational changes in secondary structure of egg albumen as a result of electrostratic interactions between egg albumen and TiO_2 NPs. The morphometric data of chicken embryo recorded a reduction at all the doses of TiO_2 NPs, but toxicity and developmental deformity (omphalocele and flexed limbs) were recorded at lower doses only. Inductively coupled plasma optical emission spectrometry (ICP-OES) confirmed presence of Ti in chicken embryos. mRNA levels of genes involved in canonical and non-canonical Wnt signaling were lowered following TiO_2 NPs treatment resulting in free radical mediated disruption of lateral plate mesoderm and somite myogenesis. Conformational changes in egg albumen and subsequent developmental deformity in chicken embryo following TiO_2 NPs treatment warrants detailed studies of NP toxicity at lower doses prior to their biomedical applications.

Nanotechnology is a rapidly expanding field, with a wide range of applications in communications, robotics, medicine, clothes, sporting goods, etc[1,2]. According to a recent survey, the number of nanotechnology-based consumer products available in the world market is more than 1800[3]. The increased use of nanomaterials is also under scrutiny due to their adverse effects on the environment, physiology and overall survival of organisms. Titanium dioxide nanoparticles (TiO_2 NPs) are the most abundantly used nano metal oxides with their documented industrial uses in pigments and additives for paints, paper, ceramics, plastics, foods, and other products. The estimated worldwide production of TiO_2 NPs is 10000 tons/year for 2011–2014 and 2.5 million metric tons/year by 2025[4]. Therefore, risk assessment studies have predicted that TiO_2 NPs will be the most prevalent nanomaterials in environment[5].

Cytotoxic potential of TiO_2 NPs is well documented in a variety of cell lines. Oxidative DNA damage and apoptosis in HepG2 cells and in human epidermal cells[6], apoptosis and/or necrosis in human astrocytoma (astrocytes-like) U87 cells[7] and mitochondrial dysfunction in BRL 3A cells[8] are some of the recent reports on cytotoxicity of TiO_2 NPs. Toxicity of TiO_2 NPs based on difference in their size has been documented in nematodes[9] and earthworm[10]. The ability of TiO_2 NPs to produce reactive oxygen species and surface charge are the reasons accredited for their toxicity[6,11]. Several engineered nanometals including TiO_2 NPs have been known to persist in the food chain and move across trophic levels resulting in various forms of toxic manifestations[11]. Hence, their effect on reproductive performance and embryonic development cannot be ignored. Accelerated hatching of larvae and deformed embryos in zebrafish[12] and histopathological changes in juvenile carp[13] are few evidences on TiO_2 NPs induced toxicity on embryonic and post-hatch development. Hatching inhibition and malformation of embryos of Abalone have been reported following TiO_2 NPs exposure[14]. Also, prenatal exposure of TiO_2 NPs in female rats impacts genes controlling brain development in offspring[15] providing compelling evidences on systemic and developmental toxicity.

[1]Department of Zoology, Faculty of Science, The M.S. University of Baroda, Vadodara, India. [2]Department of Chemistry, Faculty of Science, The M.S. University of Baroda, Vadodara, India. [3]School of Chemical sciences, Central University of Gujarat, Gandhinagar, India. Correspondence and requests for materials should be addressed to R.D. (email: rv.devkar-zoo@msubaroda.ac.in)

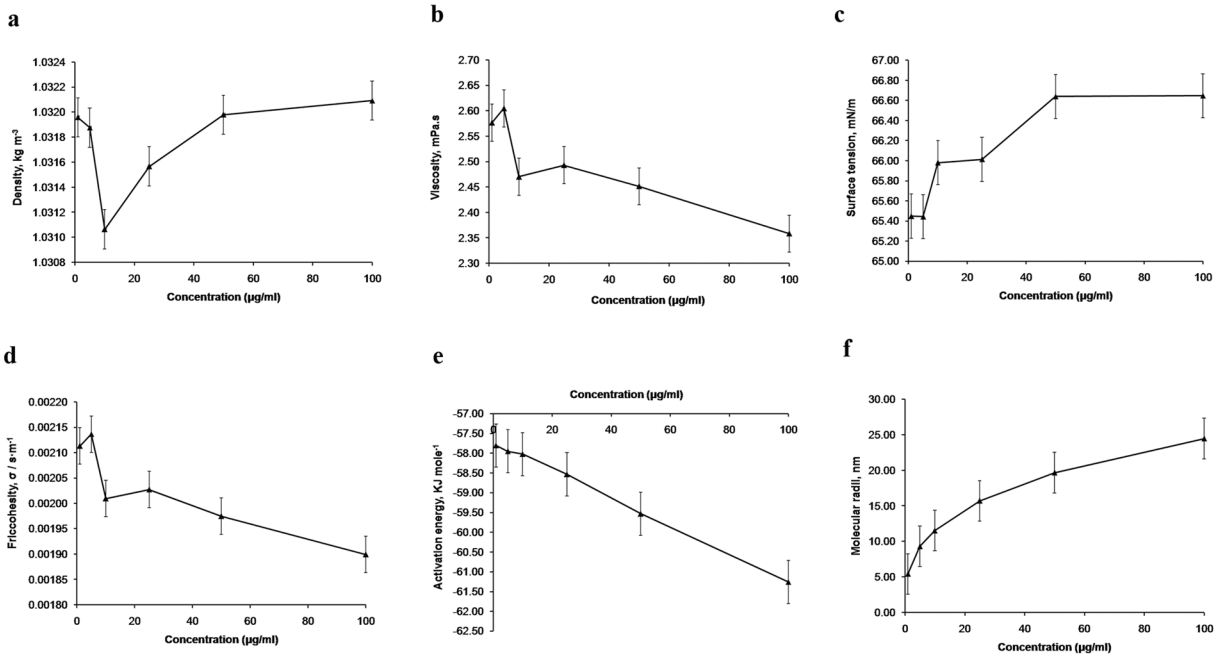

Figure 1. Physicochemical analysis of titanium dioxide nanoparticles and their interaction with egg albumen. Density, Viscosity, Surface tension, Friccohesity, Activation energy and Molecular radii of TiO_2 NPs in albumen (**a**–**f**) respectively.

Chicken embryo is a sensitive and popularly used model for assessing developmental toxicity and teratogeny of various nanoparticles. Hence, chicken embryo was chosen as an experimental model in our study to assess the impact of TiO_2 NPs on embryonic development. Other studies had reported developmental toxicity of graphite[16], copper[17], carbon[18], platinum[19], pristine graphene[20] and silver[21] nanoparticles on chicken embryo, but their *in ovo* physicochemical interactions with biomolecules such as egg albumen have not been taken into account. In the present study, we assess the interaction of TiO_2 NPs with egg albumen and its subsequent impact on chicken embryonic development.

Results

In DLS analysis, TiO_2 NPs presented a single distribution with peak centered at 88.6 nm. The plot showed that the nanoparticles have a narrow size distribution with an average diameter of about 88.6 nm (Supplementary Figure S1).

Physicochemical analysis. Results shown herein are quantification of interaction of peptide bonds with TiO_2 NPs and alteration in the Lennard Jone potential that varies spontaneity and strength of interactive force. There was a decrement in density (1.031064 $kg.m^{-3}$) of TiO_2 NPs + albumen at 10 µg/ml, whereas, 25, 50 and 100 µg/ml recorded steadily ascending values (1.031567, 1.031979 and 1.032092 $kg.m^{-3}$ respectively) (Fig. 1a and Supplementary Table S2). Lower concentrations of TiO_2 NPs (1 and 5 µg/ml) recorded higher viscosity indices (2.57 and 2.60 mPa.s). The viscosity indices of 10, 25 and 50 µg/ml doses were comparable to each other (2.47, 2.49 and 2.45 mPa.s) but, 100 µg/ml dose accounted for a decline in viscosity (2.35 mPa.s) (Fig. 1b and Supplementary Table S2). Indices of surface tension showed an increase at 10 µg/ml concentration of TiO_2 NPs (65.98 $mN.m^{-1}$) as compared to 1 and 5 µg/ml concentrations (65.45 and 65.44 $mN.m^{-1}$ respectively). However, 25, 50 and 100 µg/ml doses recorded a steady increment in surface tension (66.01, 66.64 and 66.65 $mN.m^{-1}$) (Fig. 1c and Supplementary Table S2). Friccohesity indices showed a decline at 10 µg/ml TiO_2 NPs (0.002009 $s.m^{-1}$) as compared to 1 and 5 µg/ml concentrations (0.002113 and 0.002136 $s.m^{-1}$ respectively). A steady decline in friccohesity (0.002027, 0.001974 and 0.001899 $s.m^{-1}$ at 25, 50 and 100 µg/ml doses respectively) was also observed in this study (Fig. 1d and Supplementary Table S2). A dose dependent decline in activation energy was recorded from 1–100 µg/ml doses with −57.81 $KJ.mole^{-1}$ as the highest value and −61.26 $KJ.mole^{-1}$ as the lowest value respectively (Fig. 1e and Supplementary Table S2). An increase in molecular radii (5–11.53 nm) was observed at 1–10 µg/ml TiO_2 NPs. Further, a steady increase in molecular radii (15.69, 19.66 and 24.45 nm) was observed at 25, 50 and 100 µg/ml doses respectively (Fig. 1f and Supplementary Table S2).

Spectroscopic characterization. Comparative FTIR spectra (400–4000 cm^{-1}) of native albumen and TiO_2 NPs + albumen depicting amide A (around 3400 cm^{-1}), amide B (about 3090 cm^{-1}), amide I and II (region between 1600–1700 cm^{-1}) domains are shown in Fig. 2a. The broad peak at 3591 and 3434 cm^{-1} in the amide A region of native albumen corresponds to the H-O-H asymmetric and symmetric stretching respectively whereas TiO_2 NPs + albumen recorded a shift in H-O-H stretching peak to 3478 cm^{-1}. Also, a shift in peak from 2071 cm^{-1} (in albumen) to 2083 cm^{-1} (TiO_2 NPs + albumen) was recorded. The amide I and II secondary

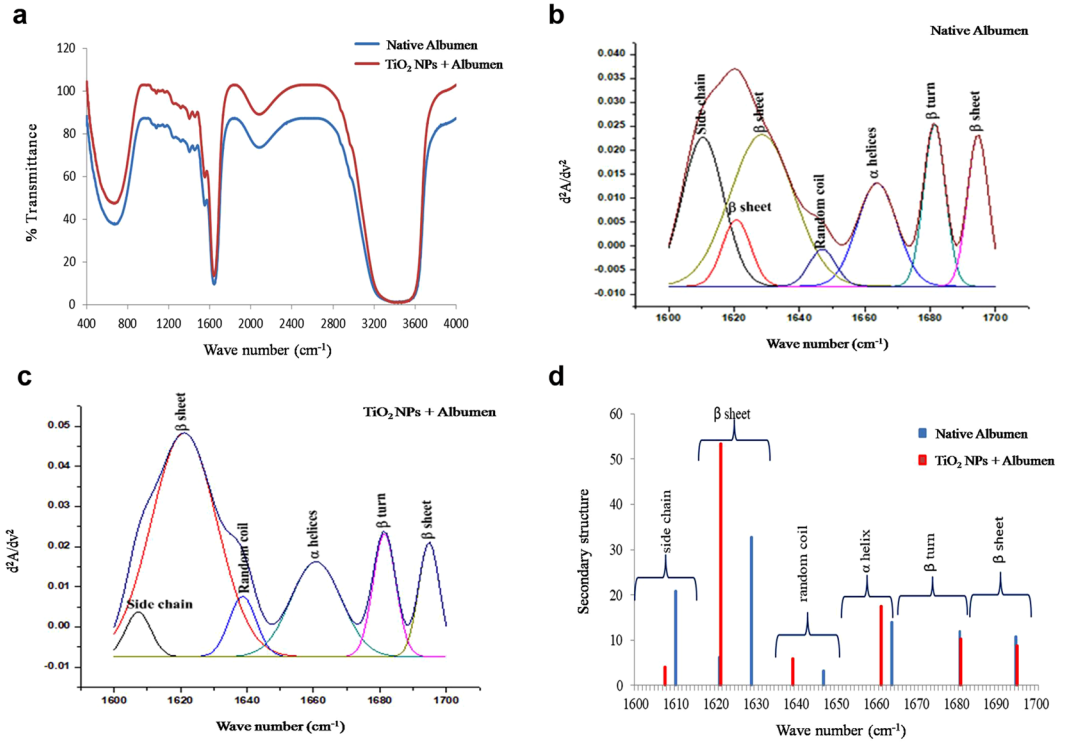

Figure 2. FTIR spectra of native egg albumen and TiO_2 NPs + Albumen. (**a**) Entire spectral range from 400–4000 cm^{-1}; (**b**–**d**) Gaussian curve fitting of secondary derivative of Native Albumen and TiO_2 NPs + Albumen with Comparative Secondary structure elements from FTIR spectra.

fingerprint regions (in albumen) recorded two peaks at 1651 cm^{-1} and 1642 cm^{-1} but in TiO_2 NPs + albumen a peak was recorded at 1641 cm^{-1}. A peak in the amide III region was recorded at 1243 cm^{-1} in albumen whereas, TiO_2 NPs + albumen recorded a shift to peak 1551 cm^{-1}. Also, peaks at 1457 and 1451 cm^{-1} in albumen and TiO_2 NPs + albumen respectively are due to $-CH_2$ scissoring vibration whereas, a peak at 675 cm^{-1} in TiO_2 NPs + albumen corresponds to Ti-O vibrational mode of TiO_2 NPs. Results obtained in deconvoluted Gaussian fitted spectra (Fig. 2b,c) and integrated peak areas of secondary-derivative structure element (Fig. 2d and Supplementary Table S3) and in albumen and TiO_2 NPs + albumen showed that albumen was mainly composed of side chain (1610 cm^{-1}, 20.93%) inter or intramolecular β sheet (1621–1629 cm^{-1}, 39.11%) closely followed by α helices (1664 cm^{-1}, 13.94%) with minor proportions of β turns (1681 cm^{-1}, 11.95%) and β sheet (1695 cm^{-1}, 10.76%). After interaction with TiO_2 NPs, a decrease in side chain (1607 cm^{-1}, 4.11%), β turns (1681 cm^{-1}, 10.31%) and β sheet (1695 cm^{-1}, 8.81%) and an increase in inter or intramolecular β sheet (1621cm^{-1}, 53.39%) and α helices (1661 cm^{-1}, 17.46%) was recorded.

Natality and Morphometry of Chick embryos. Lower doses (10 and 25 µg/ml) of TiO_2 NPs treatment accounted for 12.5% and 25% viable embryos respectively on 19th day of incubation. Also, 56.25% and 43.75% embryos were found to be malformed at 10 and 25 µg/ml doses. However, higher doses (50 and 100 µg/ml) recorded viable embryos ranging between 75–87.5% (Fig. 3a). Morphometry of the embryos (whole weight and length) recorded significant decrement at all the doses (10–100 µg/ml) (Fig. 3b). Whole weights of liver, brain and heart showed non-significant decrement at all the said doses (Supplementary Table S4).

ICP-OES analysis of embryos. After 4-days of TiO_2 NPs treatment, the contents of Ti in the chick embryo were measured by ICP-OES. Significantly high levels of Ti was detected (3 times increase) in embryos of eggs treated with 10 µg/ml TiO_2. But, higher dose (100 µg/ml) accounted for a moderate non-significant content of Ti in embryos (Fig. 3c).

Deformity. Control and TiO_2 NPs treated chick embryos were examined as per Hamburger-Hamilton standard that revealed presence of flexed limbs at 10 and 25 µg/ml doses of TiO_2 NPs (Fig. 3d). Also, omphalocele (ventral body wall defect) was observed at 10 µg/ml dose. These deformities were not seen at any of the higher doses (50 and 100 µg/ml). Further confirmation of flexed limbs of 10 and 25 µg/ml TiO_2 NPs treated embryos was obtained by alcian blue- alizarine red staining (Fig. 3e).

Expression of Wnt signaling genes. RT-PCR analysis was performed to assess the effect of TiO_2 NPs on expression of key genes of canonical (CTNNB1, PITX2 and LEF1), non-canonical Wnt/Ca^{2+} (WNT11, PRKCA and CAMK2D) and Planar Cell Polarity (ROCK1 and ROCK2) pathways associated with Wnt signaling. Expression levels of genes of canonical pathway (CTNNB1, PITX2 and LEF1) were downregulated significantly

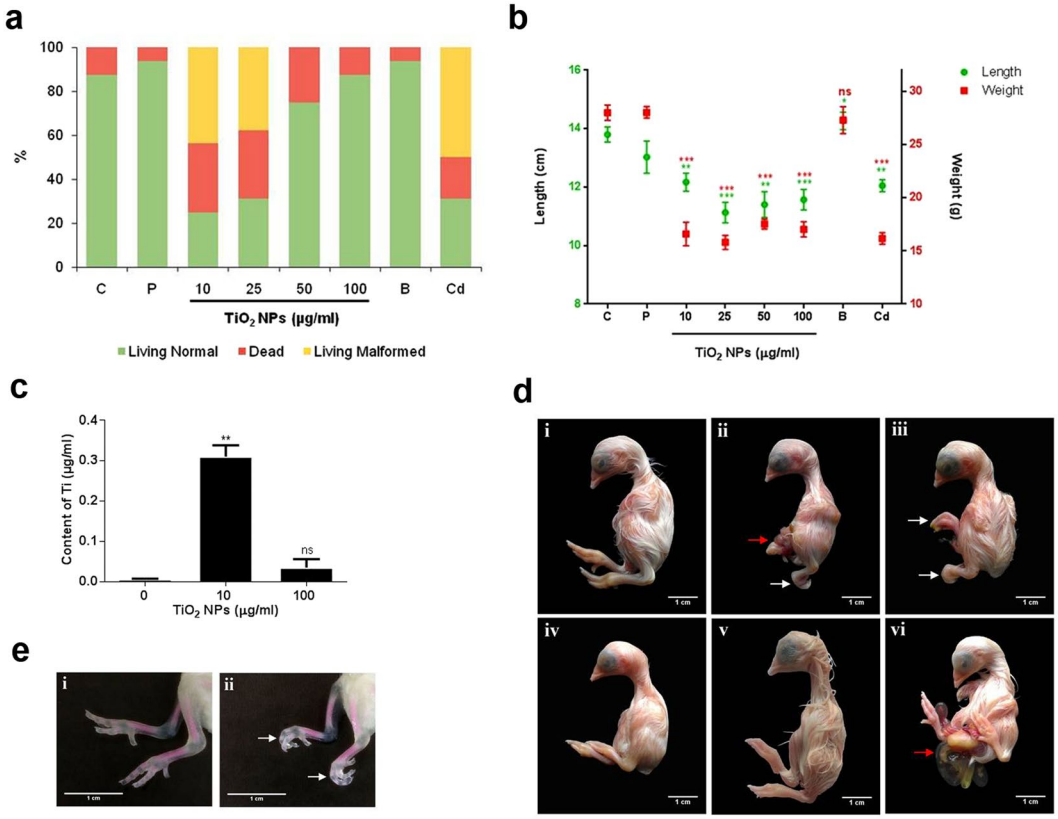

Figure 3. TiO_2 NPs induces developmental deformities in chicken embryo. (**a**) Percentages of living normal, dead and malformed embryos in 19-day-old chick embryos. (**b**) Mean body weight (g) and lengths (cm) of living 19-day-old chick embryos in control and treated groups. (**c**) Concentrations of Ti in embryos of control and TiO_2 NPs-treated group (4 day old) by ICP-OES. (**d**) Chicken-embryo development after 19 days of incubation, control (i), 10–100 µg/ml TiO_2 NPs-treated groups (ii,iii,iv), 10 µg/ml TiO_2 Bulk (v) and 10 µg/ml cadmium chloride (vi), (Scale bar: 1 cm). Embryos treated with 10 µg/ml TiO_2 NPs (ii) exhibits omphalocele (red arrow) & flexed limbs (white arrow). (**e**) Photographs showing endoskeleton (bone and cartilage) of 19-day-old chick embryos, control (i) and TiO_2 NPs–treated (ii) stained with Alizarin red S and alcian blue staining. TiO_2 NPs treated (10 µg/ml) embryos exhibits flexed digits (arrow). The data are expressed as Mean ± SD. Statistical analysis was done by one way ANOVA, $*p \leq 0.05$, $**p < 0.01$, $***p < 0.001$, ns- not significant, C- control, P-placebo, B- TiO_2 Bulk (10 µg/ml), Cd- cadmium chloride (10 µg/ml).

in embryos treated with TiO_2 NPs (10 µg/ml). A Similar trend of significant decrement was also observed in cadmium treated embryos, whereas, TiO_2 bulk treatment could not manifest any significant change (Fig. 4a–c). Expression levels of key genes of non-canonical Wnt/Ca^{2+} Wnt signaling (WNT11, PRKCA and CAMK2D) showed significantly lowered expression levels following TiO_2 NPs or cadmium treatment. However, the TiO_2 bulk treatment showed non-significant changes in the expression levels of the said genes (Fig. 4d–f). mRNA expression of key genes of Planar Cell Polarity pathway (ROCK1 and ROCK2) accounted for non-significant decrement following TiO_2 NPs or cadmium treatment. TiO_2 bulk treatment accounted for moderately significant increment in ROCK1 expression and non-significant increment in expression of ROCK2 (Fig. 4g and h). Expression levels of HOXD13 showed significantly lowered expression levels following TiO_2 NPs or cadmium treatment, whereas, the TiO_2 bulk treatment showed non-significant changes (Fig. 4i).

Somite development. It was observed that 10 µg/ml dose of TiO_2 NPs accounted for 20% decrement in the number of somites after 24 h which was comparable to that of the cadmium treated group, whereas, TiO_2 bulk treatment could not manifest any significant change (Fig. 4j).

Discussion

Nanomaterials have been reported to interact with protein molecules in unique ways and form a 'protein corona' that alters its physicochemical identity and affect its bio-distribution, kinetics and subsequent toxicity[22]. A previous study in our lab had shown that TiO_2 NPs interact with protein components of RPMI-1640 and result in higher indices of intermolecular interaction[23]. Egg albumen is reservoir of protein in an avian egg that meets the nutritional requirements of an embryo. Besides egg shell, shell membrane and chorio-allantoic membrane; egg albumen also regulates the trafficking of exogenous elements by acting as a natural biological barrier[24]. In the present study, a dose dependent increase in density of albumen was observed following addition of TiO_2 NPs. But, relatively lowest density observed at 10 µg/ml hints at effective dispersion of TiO_2 NPs in egg albumen. Higher

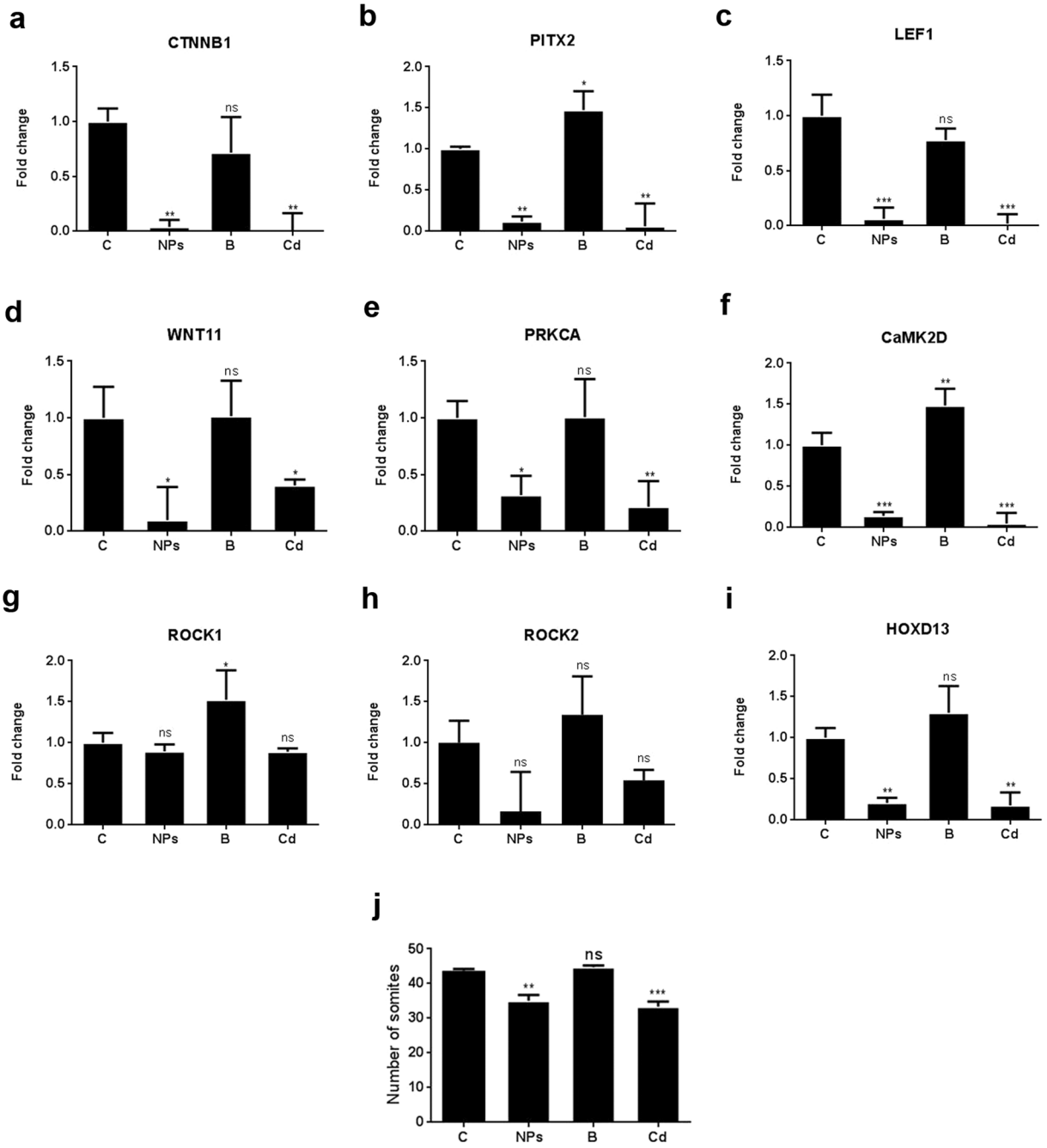

Figure 4. Expression of Wnt signaling pathway-related genes in TiO_2 NPs-treated chicken embryos. The expression of Wnt signaling pathway-related genes (**a**–**h**) including CTNNB1, PITX2, LEF1, WNT11, PRKCA, CAMK2D, ROCK1 and ROCK2 and (**i**) limb development gene HOXD13 was analyzed using reverse transcription polymerase chain reaction (RT-PCR) in control and TiO_2 NPs-treated embryos (n = 3), 4 h after treatment in shell-less culture at 60 h. All the Wnt signaling pathway related genes and limb development gene were downregulated in TiO_2 NPs-treated embryos compared to those of control embryos. *$p < 0.05$, **$p < 0.01$, ***$p < 0.001$, ns = not significant. (**j**) Somite numbers in control and TiO_2 NPs-treated embryos 24 h after treatment in shell-less culture (HH-23). There is a reduction in the number of somites in TiO_2 NPs-treated embryos as compared to the control embryos. The data are expressed as Mean ± SD. Statistical analysis was done by one way ANOVA followed by Dunnett's test. *$p < 0.05$, **$p < 0.01$, ***$p < 0.001$, ns = not significant.

intermolecular forces and cohesion are the key factors that determine viscosity and surface tension of liquids. In our study, a dose dependent decrement in viscosity and a reciprocal increment in surface tension are in support of our claim that higher intermolecular forces are as a result of higher concentration of TiO_2 NPs. Friccohesity is a product of frictional and cohesive forces within similar (protein-protein) and dissimilar (protein-nanoparticle) molecules[25]. A dose dependent decrement in friccohesity suggests weaker inter conversion between cohesive and

frictional forces implying towards a stronger nanoparticles-egg albumen interaction. Also, a decrement in activation energy is an indicator of increased proportion of collision/chemical reaction between the test compounds[23]. Relatively higher indices of activation energy recorded in TiO_2 NPs + albumen (10 µg/ml) is suggestive of more quantum of interaction between TiO_2 NPs and egg albumen. Molecular radii play an important role in dispersion of nanometals and its impact on biological systems. A dose dependent increment in molecular radii resulting due to TiO_2 NPs-egg albumen interactions implies towards formation of nanoparticle agglomerates at higher doses.

TiO_2 NPs + albumen recorded a shift in H-O-H stretching peak to 3478 cm^{-1} confirming interaction between TiO_2 NPs and albumen. Further a shift in peak from 2071 cm^{-1} (in albumen) to 2083 cm^{-1} (TiO_2 NPs + albumen) is attributable to interaction between C-O and amide groups of amino acids present in albumen. Peaks observed in the amide I and II secondary fingerprint region (in albumen) at 1651 cm^{-1} and 1642 cm^{-1} are attributable to C=O stretching and H-O-H bending respectively. However, a minor shift in C=O stretching and depletion of H-O-H bending (at 1641 cm^{-1}) was possibly on account of electrostatic interaction due to Vander Waal forces taking place between albumen and TiO_2 NPs. Peak in amide III region (at 1243 cm^{-1}) in albumen occurs due to N-H bending and C-N stretching of amino groups but, TiO_2 NPs + albumen recorded a shift (at 1551 cm^{-1}) from amide III to amide II region. This shift also portrays major conformational changes in secondary components (α helices and β sheet) of proteins possibly due to their interaction with TiO_2 NPs. Fourier-self deconvolution approach was employed to assess secondary conformational changes in amide I and II region. Venyaminov and Kalnin[26] had reported that amide peak at 1610 ± 4 corresponds to NH bending of $CO\text{-}NH_2$ bond in glutamine. In our study, amide peak at 1610 cm^{-1} in TiO_2 NPs + albumen indicates possible deformity of glutamate in egg albumen. Role of glutamate in nutrition and metabolism is well reported[27] and hence impact of structurally altered glutamate on developing chicken embryo is postulated herein. Further, an increase in β sheet and α helices in TiO_2 NPs + albumen are possibly due to TiO_2 NPs mediated conformational changes, formation of aggregates or amyloids with protein moieties in egg albumen. These findings are the first to showcase interaction of TiO_2 NPs with egg albumen and the said physicochemical alterations.

Interaction of TiO_2 NPs with egg albumen prompted us to assess its impact on embryonic development using chicken egg as a model. Significant reduction in morphometric indices (body weight and length) and higher percentage mortality was recorded in developing chicken embryos at lower doses of TiO_2 NPs (10 µg/ml). But, the higher doses of TiO_2 NPs (50 or 100 µg/ml) failed to elicit a dose-dependent toxicological response possibly because TiO_2 NPs underwent physicochemical alterations as evidenced by relatively higher indices of density, viscosity and friccohesity coupled with lower activation energy hinting at formation of NP agglomerates. Whereas, lower extent of NP-egg albumen interactions observed at 10 µg/ml of TiO_2 NPs was instrumental in its effective bio-distribution and manifested said toxicity. Percentage mortality of bulk TiO_2 treated chicken embryos was comparable to that of higher doses (50 or 100 µg/ml) of TiO_2 NPs thus providing conclusive evidence that an altered physicochemical identity of NPs failed to induce a dose dependent toxicity in chicken embryos. Nanoparticles are known to cross biological barriers like the blood brain barrier and blood placenta barrier[28]. The results obtained herein indicate that the TiO_2 NPs could cross biological barriers within an avian egg and reach the embryo. The same was confirmed by ICP-OES studies that revealed presence of higher levels of TiO_2 NPs in the embryonic tissue at the lower dose (10 µg/ml).

Omphalocele is a ventral body wall defect and is accompanied by herniation of midgut into the abdominal cavity, failure in fusion of the anterior abdominal wall with 1/3000 frequency of occurrence in human population[29]. Teratogenic agents such as cadmium[30], specific radiations[31], fungal toxins[32], etc. are known to induce omphalocele in various animal models. However, no known nanomaterials have been reported to induce omphalocele. Wnt signaling pathway has been implicated in various events of embryonic development such as cell differentiation, survival, migration, proliferation, adhesion and somite formation[33]. Canonical Wnts relay their signal via ß-Catenin pathway that control cell fate determination[33]. Whereas, the non-canonical Wnt signaling either through Wnt/Ca^{2+} pathway or planar cell polarity pathway that controls cell adhesion and movement[33]. Results obtained herein were compared with cadmium induced omphalocele chicken embryo model[30]. PITX2, a bicoid-type homeodomain transcription factor, has known to be regulated by ß-Catenin dependent Wnt pathway[34]. In the Wnt/ß-Catenin pathway, the accumulation of ß-Catenin in the nucleus converts DNA-binding factor, lymphoid enhancing factor-1 (LEF1), to a transcriptional activator and is regulated through direct physical interaction with PITX2 and ß-Catenin[35]. In this study, downregulation in expression levels of CTNNB1, PITX2 and LEF1 following TiO_2 NPs treatment (10 µg/ml) could be a key factor in the disruption of somite myogenesis by inhibiting Wnt/ß-Catenin pathway. It has been postulated that cells from somites migrate into the parietal layer of lateral plate mesoderm (LPM) to assist in forming the lateral body folds[36]. PITX2 is known to regulate cell survival[37] and its downregulation may induce abnormal apoptosis in the somite and LPM that could further interfere with the movement of the lateral body wall folds[29]. These results justify the decrement in somite count obtained in our study following TiO_2 NPs treatment (10 µg/ml). WNT11, a member of the noncanonical Wnts, is an important epithelialization factor acting on the dermomyotome whereas, PRKCA and CaMK2D control actin-cytoskeleton organization and cell contractility[33,38]. Previous studies had implicated PRKCA and CaMK2D (activated by WNT11) in the regulation of cell-cell adhesion molecules (CAMs) such as cadherins. The resultant linkages between E-cadherin and actin filaments reinforce the cell-cell junctional connection[39]. In our study, downregulation of WNT11, PRKCA and CaMK2D genes after TiO_2 NPs treatment (10 µg/ml) possibly interfered with actin-cytoskeleton organization, cell movement and cell adhesion, thus disrupting noncanonical Wnt/Ca^{2+} signaling that resulted in omphalocele. Rho kinases (ROCK) are involved in the regulation of various cellular functions (contraction, adhesion, migration, proliferation and apoptosis) including tissue closure during embryonic development. ROCK1 and ROCK2 mediate signaling from Rho to the actin cytoskeleton in the Wnt non-canonical pathway[40]. ROCK1 knockout (KO), ROCK2 KO, and ROCK1/2 double heterozygous mice has been reported to exhibit omphalocele phenotype due to disorganization of actin filament in the epithelial cells of umbilical ring[41]. Downregulation of ROCK genes following TiO_2 NPs treatment possibly disrupted actomyosin

assembly, resulting in the failure of ventral body wall closure resulting in omphalocele. Defects in ventral body wall closure and omphalocele has also been reported with accompanying limb deformities in genetically modified experimental models[42]. *Hox* genes are important regulators of limb pattern in vertebrate development, HOXD13 misexpression in the hindlimb results in shortening of the long bones, including the femur, the tibia, the fibula and the tarsometatarsals[43]. In our study, significantly lowered expression of HOXD13 in TiO_2 NPs treated embryos corroborate with the observed omphalocele. Cadmium is known to use Ca^{2+} ion channels and membrane transporters to enter in to the cells of a developing embryo. Further, it disrupts lateral plate mesodermal cells and induces omphalocele[30]. Therefore, cadmium treated chicken embryos were used as a disease control in our study wherein; expression levels of key genes of the Wnt signaling pathways were comparable to TiO_2 NP treated embryos. TiO_2 NPs are also known to cause free radicals induced cellular damage[6]. Free radical induced disruption of lateral plate mesoderm and somite myogenesis culminating in omphalocele in TiO_2 NPs treated chicken embryos is hypothesized in our study.

Besides their widespread industrial use, TiO_2 NPs have gained prominence in biomedical applications due to their long term photostability, superior biocompatibility, catalytic efficiency and a strong oxidizing power[44,45]. Photodynamic therapy for cancer, cell imaging, genetic engineering, drug delivery and biosensors are some of the reported biomedical applications of TiO_2 NPs[44,45]. Also, their use in diagnosis of cardiovascular diseases, diabetes mellitus, cancer and orthopaedic disorders underlines their prominence. But, omphalocele formation only at sub lethal (lower) concentrations reported herein raises concerns of toxicity benchmarks impacting foetal development. Hence, it raises an urge to study interactions of nanoparticles with biomolecules vis-à-vis particle size or surface modifications prior to their use in diagnostics or biomedical applications.

Conclusion

Nanometal oxides witness a wide range of biomolecules in a physiological environment that can alter their behavior and responses. In the present study, TiO_2 NPs were found to interact with egg albumen as evidenced by changes in their proteinic secondary structure. These interactions could possibly allow TiO_2 NPs to traverse the biological barriers (shell membrane and CAM) within chicken egg and affect the growth and development of embryos and cause malformations like omphalocele and flexed limbs. Also, the observed mortality and significant decrement in morphometry (whole weight and length) are attributable to TiO_2 NPs-albumen interactions. Omphalocele formation in TiO_2 NPs treated groups is possibly due to the disruption of somite myogenesis as evidenced by alterations in expression of key genes of Wnt signaling pathway. Hence, use of TiO_2 NPs in diagnostics and therapy warrants a detailed research in embryos by taking into account its particle size, surface modifications and interaction with biomolecules.

Materials and Methods

Availability of Data and Materials. The datasets supporting the conclusions of this article are included within the article.

Nanoparticles. Titanium (IV) oxide nanopowder (TiO_2 NPs, mixture of Anatase and rutile, Cat. no. 634662, particle size <100 nm, 99.5% purity) was procured from Aldrich (St. Louis, MO, USA). TiO_2 NPs (1 mg/ml) were suspended in water and probe sonicated (LMUC-4, Labman scientific instruments Pvt. Ltd., Kolkata, India) for 30 min. After sonication, the particle size distribution was measured using a 90 plus DLS (Dynamic light scattering) unit from Brookhaven (Holtsville, USA).

Physicochemical analysis. The physicochemical properties such as density, viscosity, surface tension, activation energy, friccohesity and molecular radii were assessed in absence or presence of TiO_2 NPs in egg albumen (freshly collected). TiO_2 NPs were suspended in egg albumen at 1, 5, 10, 25, 50 and 100 μg/ml concentrations. Density of TiO_2 NPs in water and egg albumen were determined with Anton Paar Density and Sound velocity Meter (DSA 5000 M). Density was calculated using equation 1:

$$\rho = \rho^{\circ} + S_{\rho}m + S'_{\rho}m^2 \tag{1}$$

(ρ° at $m \rightarrow 0$ is limiting density, $S\rho$ is the 1st slope)

Viscosity was measured as viscous flow times (VFT) using Borosil Mansingh Survismeter[23] at physiological temperature of 37 °C (LAUDA ALPHA RA 8 thermostat) and calculated by equation 2:

$$\eta = \left(\frac{t}{t_{\circ}}\right)\left(\frac{\rho}{\rho_{\circ}}\right)\eta_{\circ} \tag{2}$$

($\eta_{\circ}$ is viscosity of water and $t_{\circ}$, t are flow times of solvent and mixtures respectively)

The η data were regressed with following equation 3:

$$\eta = \eta^{\circ} + S_{\eta}m \tag{3}$$

(η° atm $\rightarrow 0$ is limiting viscosity; S_{η} is the 1st degree slope).

Surface tension was measured by counting pendent drop numbers (PDN) using Borosil Mansingh Survismeter and calculated by equation 4:

$$\gamma = \left(\frac{\eta_{\circ}}{\eta}\right)\left(\frac{\rho_{\circ}}{\rho}\right)\gamma_{\circ} \tag{4}$$

($\gamma_\circ$ is surface tension of water, $\eta_\circ$ and η are pendent drop numbers of medium and solutions respectively)
The γ data were regressed for limiting values γ° at $m \rightarrow 0$ with following equation 5:

$$\gamma = \gamma^\circ + S_\gamma m \tag{5}$$

(γ° is limiting surface tension, and S_γ is the 1st degree slope)
Friccohesity was calculated using Mansingh equation 6[46]:

$$\sigma = \sigma_\circ \left[\left(\frac{t}{t_\circ} \pm \frac{B}{t} \right) \left(\frac{\eta}{\eta_\circ} \pm 0.0012(1 - p) \right) \right] \tag{6}$$

(σ is friccohesity, t and $t_\circ$ are the sample and solution viscous flow times respectively, $\eta_\circ$ and η are the pendant drop numbers of medium and solutions respectively)
Reference friccohesity was calculated by equation 7

$$\sigma_\circ = \eta_\circ / \gamma_\circ \tag{7}$$

where, $\eta_\circ$ and $\gamma_\circ$ are the viscosity and surface tension of references respectively.
For activation energy, the partial molar volume V_2 was calculated with following equation 8:

$$V_2 = \left[\frac{1000(\rho^\circ - \rho)}{m\rho^\circ \rho} \right] + \frac{M}{\rho} \tag{8}$$

(M is molar mass, ρ° is density of water and ρ is density of solution)
The V_1 for water or albumen at 37 °C is calculated with equation 9:

$$V_1 = \frac{M}{\rho} \tag{9}$$

V_1 and V_2 are used for calculating activation energy by using equation 10:

$$\Delta\mu_1^* = RT \ln \left(\frac{\eta_\circ V_1}{hN} \right) \tag{10}$$

($\Delta\mu_1^*$ is activation energy of water or albumen, R is gas constant, h is Planck constant and N is Avogadro number (6.023×10^{23}). Activation energy ($\Delta\mu_2^*$J/mol) was calculated by using equation 11:

$$\Delta\mu_2^* = \Delta\mu_1^* - \left[\left(\frac{RT}{V_2} \right) ((1000\eta) - (V_1 - V_2)) \right] \tag{11}$$

Molecular radii r (nm) is calculated by using equation 12:

$$r = \sqrt[3]{\frac{3\phi}{4\pi Nc}} \tag{12}$$

(ϕ is volume fraction of water or albumen entangled with NPs, N is Avogadro number, c is concentration and π is constant).
Each parameter was measured in triplicates.

Spectroscopic characterization. Protein-nanoparticle interaction was identified by Fourier transform infrared (FTIR) spectra (PerkinElmer spectrum 65 series, PerkinElmer, Inc., MA, USA). Sample was prepared by making pellet of 1.5 to 2 mg of sample mixed with 200 mg KBr (AR, Sigma, USA) in the KBr press machine (model Mp-15) at 5 kg/cm^2 pressure for 2 min. After taking background scan, samples were analyzed at 400–4000 cm^{-1}. FTIR direct-transmittance spectroscopy (KBr) was used to indicate the degree to which oxygen groups were removed and the IR absorption of water from the air was mostly eliminated. Each measurement was repeated in triplicates to minimize the error.

Chicken Embryo model and experimental groups. The experimental protocol (MSU-Z/IAEC/03-2017) was approved by the Institutional Animal Ethical Committee (IAEC) and the Committee for the Purpose of Control and Supervision of Experiments on Animals (827/GO/Re/S/04/CPCSEA). Fertilized eggs (55 ± 2.1 g) of White leghorn (*Gallus gallus domesticus*) were obtained from Shakti hatcheries, Sarsa, Gujarat, stored for 2 days at 12 °C and then incubated under standard conditions (37.5 °C, humidity 60%) for 48 hours and guidelines of Committee for the Purpose of Control and Supervision of Experiments on Animals (CPCSEA) were hereby followed for all the experiments conducted on the chicken embryo. The procedures for *in ovo* experimentation were as per the standard operating protocols of our laboratory. Candling was done to confirm the fertility of eggs and unfertile eggs were discarded. Eggs were randomly divided into six groups of 16 eggs/group viz. control (untreated), placebo (treated with PBS) and TiO_2 treated (10, 25, 50 and 100 µg/ml) groups. TiO_2 NPs powder was suspended in saline (1 mg/ml) and sonicated (LMUC-4, Labman scientific instruments Pvt. Ltd. Kolkata, India) for 30 min. Further, TiO_2 NPs were diluted to 10, 25, 50 and 100 µg/ml doses. Test samples were injected *in ovo* (0.3 ml/egg) in airspace using sterile 1 ml tuberculin syringe and incubated for 18 days.

Gene	Gene Name	Accession number	Primer Sequence (5′-3′)
GAPDH	Glyceraldehyde 3-phosphate dehydrogenase	NM_204305.1	F:-ACTGTCAAGGCTGAGAACGG R:-ACCTGCATCTGCCCATTTGA
HOXD13	Homeobox D-13	NM_205434.1	F:-TCTGGCTAATGGCTGGAACG R:-ATCTCGGGCTGGTTTAGTGC
CTNNB1	ß-catenin	NM_205081.1	F:-GTCCTGTATGAGTGGGAGCA R:-GTTTCGGGGAACATAGCAGAA
PITX2	Paired-like homeodomain 2	NM_205010.1	F:-CGATGAGTTGCATGAAGGAC R:-AGGAGGAAGGTGAGGAGGAG
LEF1	Lymphoid enhancer-binding factor 1	XM_015276137.1	F:-TCACCTACAGCGATGAGCAC R:-TATCAGGAGCTGGAGGATGC
WNT11	Wingless-type MMTV integration site family, member 11	XM_015280851.1	F:-TTCATCTTTGGCCCTGAATC R:-AGCTCGATGGATGAGCAGTT
PRKCA	Protein kinase C	XM_004946229.2	F:-ACAACCAGGACCTTCTGTGG R:-TCTCGTAGAGCAGCACTCCA
CAMK2D	Calcium/calmodulin-dependent protein kinase II delta	XM_015276279.1	F:-GCCAATCCACACCATTATCC R:-CCATCCATGTACTGCGTGAG
ROCK1	Rho-associated, coiled-coil containing protein kinase 1	XM_015277931.1	F:-TGACTGGTGGTCAGTTGGAG R:TAGAGATCTCGTTGTCATCAGG
ROCK2	Rho-associated, coiled-coil containing protein kinase 2	XM_015276085.1	F:-GACTGGTGGTCCGTAGGAGT R:-GCAGTCTCTCGGATGTTGTC

Table 1. Primers used for RT-PCR.

Autopsy, morphometry and staining. On 19th day, the experiment was terminated by opening the eggs and the viable embryos were weighed and decapitated. The morphology of the embryos was examined according to the Hamburger and Hamilton[47] standards and ratios of live vs. dead/malformed were recorded. Deformities of the head, limbs, body and tail were observed under a dissecting microscope and photographed with a digital (Nikon coolpix p900) camera. Two embryos per group were processed for Alizarine-alcian blue staining[48]. Briefly, skin and viscera was removed and embryos were fixed in 96% ethanol for 3 days followed by acetone for 2 days. Later, embryos were then rinsed in ethanol for 1–2 h and stained with Alizarine-alcian blue stain (0.015% Alcian blue, 0.005% Alizarin red in 70% ethanol, 20% acetic acid and 10% dH_2O) at 37 °C for 4 h. Embryos were rinsed in ethanol and running tap water for one hour each and muscles were cleared in an aqueous solution of 1% potassium hydroxide. De-staining of embryos was done in a graded series of glycerol/potassium hydroxide (20% glycerol/0.8% KOH, 50% glycerol/ 0.5% KOH and 80% glycerol/0.2% KOH respectively) and stored in 100% glycerol.

Inductively coupled plasma optical emission spectroscopy (ICP-OES). Four days old control and treated eggs (three per group) were opened and embryos were digested overnight at 40 °C in 6 ml of conc. nitric acid and 3 ml of hydrogen peroxide. Contents were heated in an oven (110 °C) for 2 h, cooled at room temperature and diluted with 11 ml of dH_2O. The concentrations of nanosized particles in the embryo were quantified by ICP-OES[49].

Shell-less culture and dosing. In a separate set of experiment, procured eggs were incubated for 60 h in standard conditions and later were explanted into shell-less culture as per Dugan, *et al.*[50]. The embryos were divided into four groups of six eggs each viz control (50 µl PBS), positive control (50 µl of 50 µM $CdCl_2$), TiO_2 NPs treated (50 µl of 10 µg/ml) and bulk TiO_2 (50 µl of 10 µg/ml). Dosing was done directly on blastodisc using a micropipette and embryos were incubated for 4 h or 24 h.

Autopsy, RNA isolation and qPCR study. Developing embryonal discs (three per group, HH 17; whole embryo) were transferred in RNA later solution (Invitrogen, California, USA). Total RNA was isolated using TRIzol reagent (Invitrogen, California, USA) and cDNA was synthesized by reverse transcription of 1 µg of total RNA using iScript cDNA Synthesis kit (BIORAD, California, USA). For HOXD13, total RNA was isolated from limb bud of 4 day old control and treated embryos. Quantitative RT-PCR was performed using SYBR Select Master Mix (Applied Biosystems) in QuantStudio12K (Life Technologies) real-time PCR machine with primers (Table 1) to detect selected messenger RNA (mRNA) targets. The relative mRNA expression levels were normalized against expression levels of GAPDH for each sample and analyzed using $2^{-\Delta\Delta CT}$ method[51].

Somite development. The embryos (three per group) were dissected from their membranes 24 hours after treatment (HH 23) and inspected using the dissecting microscope to count somite numbers.

Statistical analysis. Data analysis was carried out by unpaired Student's t-test or one way analysis of variance (ANOVA) using Graph Pad Prism 6.0 (CA, USA). Differences between control and treatment groups were deemed to be significant when $P < 0.05$.

References

1. Oberdörster, G., Oberdörster, E. & Oberdörster, J. Nanotoxicology: an emerging discipline evolving from studies of ultrafine particles. *Environmental health perspectives* **113**, 823 (2005).
2. Nel, A., Xia, T., Mädler, L. & Li, N. Toxic potential of materials at the nanolevel. *science* **311**, 622–627 (2006).

3. Vance, M. E. *et al*. Nanotechnology in the real world: Redeveloping the nanomaterial consumer products inventory. *Beilstein journal of nanotechnology* **6**, 1769 (2015).
4. Dalai, S., Pakrashi, S., Chandrasekaran, N. & Mukherjee, A. Acute toxicity of TiO2 nanoparticles to Ceriodaphnia dubia under visible light and dark conditions in a freshwater system. *PLoS One* **8**, e62970 (2013).
5. Maurer-Jones, M. A., Gunsolus, I. L., Murphy, C. J. & Haynes, C. L. Toxicity of engineered nanoparticles in the environment. *Analytical chemistry* **85**, 3036–3049 (2013).
6. Shukla, R. K. *et al*. TiO2 nanoparticles induce oxidative DNA damage and apoptosis in human liver cells. *Nanotoxicology* **7**, 48–60 (2013).
7. Lai, J. C. *et al*. Exposure to titanium dioxide and other metallic oxide nanoparticles induces cytotoxicity on human neural cells and fibroblasts. *International journal of nanomedicine* **3**, 533 (2008).
8. Hussain, S., Hess, K., Gearhart, J., Geiss, K. & Schlager, J. *In vitro* toxicity of nanoparticles in BRL 3A rat liver cells. *Toxicology in vitro* **19**, 975–983 (2005).
9. Li, Y. *et al*. Molecular control of TiO2-NPs toxicity formation at predicted environmental relevant concentrations by Mn-SODs proteins. *PLoS One* **7**, e44688 (2012).
10. Hu, C. *et al*. Toxicological effects of TiO 2 and ZnO nanoparticles in soil on earthworm Eisenia fetida. *Soil Biology and Biochemistry* **42**, 586–591 (2010).
11. Gupta, G. S., Kumar, A., Shanker, R. & Dhawan, A. Assessment of agglomeration, co-sedimentation and trophic transfer of titanium dioxide nanoparticles in a laboratory-scale predator-prey model system. *Scientific reports* **6**, 31422 (2016).
12. Clemente, Z., Castro, V., Moura, M., Jonsson, C. & Fraceto, L. Toxicity assessment of TiO 2 nanoparticles in zebrafish embryos under different exposure conditions. *Aquatic toxicology* **147**, 129–139 (2014).
13. Linhua, H., Zhenyu, W. & Baoshan, X. Effect of sub-acute exposure to TiO2 nanoparticles on oxidative stress and histopathological changes in Juvenile Carp (Cyprinus carpio). *Journal of Environmental Sciences* **21**, 1459–1466 (2009).
14. Zhu, X., Zhou, J. & Cai, Z. TiO2 nanoparticles in the marine environment: Impact on the toxicity of tributyltin to abalone (Haliotis diversicolor supertexta) embryos. *Environmental science & technology* **45**, 3753–3758 (2011).
15. Mohammadipour, A. *et al*. Maternal exposure to titanium dioxide nanoparticles during pregnancy; impaired memory and decreased hippocampal cell proliferation in rat offspring. *Environmental toxicology and pharmacology* **37**, 617–625 (2014).
16. Wierzbicki, M., Sawosz, E. & Grodzik, M. Caveolin-1 localization in chicken embryo chorioallantoic membrane treated with diamond and graphite nanoparticles. *Brzozowski m., głogowski r., grzeszczak-pytlak a. Reproduc-tive efficiency of mink females, selected for weaned litter size after first season of repro-duction* **5**, 133 (2012).
17. Pineda, L., Sawosz, E., Vadalasetty, K. & Chwalibog, A. Effect of copper nanoparticles on metabolic rate and development of chicken embryos. *Animal feed science and technology* **186**, 125–129 (2013).
18. Wierzbicki, M. *et al*. Carbon nanoparticles downregulate expression of basic fibroblast growth factor in the heart during embryogenesis. *International journal of nanomedicine* **8**, 3427 (2013).
19. Prasek, M. *et al*. Influence of nanoparticles of platinum on chicken embryo development and brain morphology. *Nanoscale research letters* **8**, 251 (2013).
20. Szmidt, M. *et al*. Toxicity of different forms of graphene in a chicken embryo model. *Environmental Science and Pollution Research* **23**, 19940–19948 (2016).
21. Hotowy, A. *et al*. Silver nanoparticles administered to chicken affect VEGFA and FGF2 gene expression in breast muscle and heart. *Nanoscale research letters* **7**, 418 (2012).
22. Walkey, C. D. & Chan, W. C. Understanding and controlling the interaction of nanomaterials with proteins in a physiological environment. *Chemical Society Reviews* **41**, 2780–2799 (2012).
23. Patel, S. *et al*. DNA binding and dispersion activities of titanium dioxide nanoparticles with UV/vis spectrophotometry, fluorescence spectroscopy and physicochemical analysis at physiological temperature. *Journal of Molecular Liquids* **213**, 304–311 (2016).
24. Willems, E., Decuypere, E., Buyse, J. & Everaert, N. Importance of albumen during embryonic development in avian species, with emphasis on domestic chicken. *World's poultry science journal* **70**, 503–518 (2014).
25. Singh, M. Study of apparent molal volume and viscosity of mutual citric acid and disodium hydrogen orthophosphate aqueous systems. *Journal of Chemical Sciences* **118**, 269–274 (2006).
26. Venyaminov, S. Y. & Kalnin, N. Quantitative IR spectrophotometry of peptide compounds in water (H2O) solutions. II. Amide absorption bands of polypeptides and fibrous proteins in α-, β-, and random coil conformations. *Biopolymers* **30**, 1259–1271 (1990).
27. Brosnan, J. T. & Brosnan, M. E. Glutamate: a truly functional amino acid. *Amino acids* **45**, 413–418 (2013).
28. Rollerova, E. *et al*. Titanium dioxide nanoparticles: some aspects of toxicity/focus on the development. *Endocrine regulations* **49**, 97–112 (2015).
29. Doi, T., Puri, P., Bannigan, J. & Thompson, J. Altered PITX2 and LEF1 gene expression in the cadmium-induced omphalocele in the chick model. *Pediatric Surgery International* **27**, 495–499 (2011).
30. Thompson, J. M. & Bannigan, J. G. Omphalocele induction in the chick embryo by administration of cadmium. *Journal of pediatric surgery* **42**, 1703–1709 (2007).
31. Pampfer, S. & Streffer, C. Prenatal death and malformations after irradiation of mouse zygotes with neutrons or X-rays. *Teratology* **37**, 599–607 (1988).
32. Wangikar, P., Dwivedi, P. & Sinha, N. Effect in rats of simultaneous prenatal exposure to ochratoxin A and aflatoxin B1. I. Maternal toxicity and fetal malformations. *Birth defects research Part B: Developmental and reproductive toxicology* **71**, 343–351 (2004).
33. Doi, T., Puri, P., Bannigan, J. & Thompson, J. Disruption of noncanonical Wnt/CA 2+ pathway in the cadmium-induced omphalocele in the chick model. *Journal of pediatric surgery* **45**, 1645–1649 (2010).
34. Kioussi, C. *et al*. Identification of a Wnt/Dvl/β-Catenin → Pitx2 pathway mediating cell-type-specific proliferation during development. *Cell* **111**, 673–685 (2002).
35. Vadlamudi, U. *et al*. PITX2, β-catenin and LEF-1 interact to synergistically regulate the LEF-1 promoter. *Journal of cell science* **118**, 1129–1137 (2005).
36. Burke, A. C. & Nowicki, J. A new view of patterning domains in the vertebrate mesoderm. *Developmental cell* **4**, 159–165 (2003).
37. Shih, H. P., Gross, M. K. & Kioussi, C. Cranial muscle defects of Pitx2 mutants result from specification defects in the first branchial arch. *Proceedings of the National Academy of Sciences* **104**, 5907–5912 (2007).
38. Geetha-Loganathan, P., Nimmagadda, S., Huang, R., Christ, B. & Scaal, M. Regulation of ectodermal Wnt6 expression by the neural tube is transduced by dermomyotomal Wnt11: a mechanism of dermomyotomal lip sustainment. *Development* **133**, 2897–2904 (2006).
39. Ozaki, M., Ogita, H. & Takai, Y. Involvement of integrin-induced activation of protein kinase C in the formation of adherens junctions. *Genes to Cells* **12**, 651–662 (2007).
40. Shi, J. & Wei, L. Rho kinase in the regulation of cell death and survival. *Archivum immunologiae et therapiae experimentalis* **55**, 61–75 (2007).
41. Shimizu, Y. *et al*. ROCK-I regulates closure of the eyelids and ventral body wall by inducing assembly of actomyosin bundles. *J Cell Biol* **168**, 941–953 (2005).
42. Matsumaru, D. *et al*. Genetic analysis of Hedgehog signaling in ventral body wall development and the onset of omphalocele formation. *PloS one* **6**, e16260 (2011).

43. Goff, D. J. & Tabin, C. J. Analysis of Hoxd-13 and Hoxd-11 misexpression in chick limb buds reveals that Hox genes affect both bone condensation and growth. *Development* **124**, 627–636 (1997).
44. Wu, S., Weng, Z., Liu, X., Yeung, K. & Chu, P. Functionalized TiO2 based nanomaterials for biomedical applications. *Advanced Functional Materials* **24**, 5464–5481 (2014).
45. Yin, Z. F., Wu, L., Yang, H. G. & Su, Y. H. Recent progress in biomedical applications of titanium dioxide. *Physical Chemistry Chemical Physics* **15**, 4844–4858 (2013).
46. Chandra, A., Patidar, V., Singh, M. & Kale, R. Physicochemical and friccohesity study of glycine, L-alanine and L-phenylalanine with aqueous methyltrioctylammonium and cetylpyridinium chloride from T = (293.15 to 308.15) K. *The Journal of Chemical Thermodynamics* **65**, 18–28 (2013).
47. Hamburger, V. & Hamilton, H. L. A series of normal stages in the development of the chick embryo. *Journal of morphology* **88**, 49–92 (1951).
48. Lamb, K. J. *et al*. Diverse range of fixed positional deformities and bone growth restraint provoked by flaccid paralysis in embryonic chicks. *International journal of experimental pathology* **84**, 191–199 (2003).
49. Bryszewska, M. A., Hannam, S. E., Olivas, R. M. & Camara, C. Direct arsenic determination in exposed embryos of zebrafish (Danio rerio) with Zeeman electrothermal atomic absorption spectrophotometry. *Spectroscopy Letters* **42**, 363–369 (2009).
50. Dugan, J. D., Lawton, M. T., Glaser, B. & Brem, H. A new technique for explantation and *in vitro* cultivation of chicken embryos. *The Anatomical Record* **229**, 125–128 (1991).
51. Livak, K. J. & Schmittgen, T. D. Analysis of relative gene expression data using real-time quantitative PCR and the $2-\Delta\Delta CT$ method. *methods* **25**, 402–408 (2001).

Acknowledgements

The authors are thankful to Science and Engineering Research Board (SERB-DST) for financial support in form of Major Research Project (SR/SO/AS-45/2011; 2012–2015). Co-ordinator, DBTMSUB-ILSPARE (for technical support), Ms. Dhruva Trivedi (photo-editing), Mr. Dilip Patil (Rubamin Limited, Vadodara for ICP-OES), Ms. Kavita Shirsath and Mr Kapil Upadhyay (technical help) are also acknowledged.

Author Contributions

R.D. conceptualized the idea and with S.P. designed the study. S.P. and S.J. conducted experiments on chick embryo toxicity whereas, R.C. performed physicochemical studies and later, M.S., and R.C. did data analysis. R.D., S.P. and M.S. drafted the manuscript with inputs from S.T., S.J. and R.C. All authors gave intellectual input to the study and approved the final version of the manuscript.

Additional Information

Supplementary information accompanies this paper at https://doi.org/10.1038/s41598-018-23215-7.

Competing Interests: The authors declare no competing interests.

Publisher's note: Springer Nature remains neutral with regard to jurisdictional claims in published maps and institutional affiliations.